THERMAL ASPECTS FOR COMPOSITE STRUCTURES - FROM MANUFACTURING TO IN-SERVICE PREDICTIONS

T. Sproewitz*, **J. Tessmer*** and **T. Wille***
*DLR, Institute of Composite Structures and Adaptive Systems
Lilienthalplatz 7, 38108 Braunschweig, Germany
Mail: tom.sproewitz@dlr.de, Phone: +49-(0)531-295-2288, FAX: +49-(0)531-295-2232

Keywords: *composites, CTE, process simulation, shrinkage, spring-in, thermo-elastic*

Abstract

In this paper a simulation strategy for composite structures will be presented taking into account all thermal aspects, which may occure from manufacturing to in-service. Focus herein is laid on the thermo-elastic simulation of the spring-in effect on large airframe structures based on the FE-method. Besides the identification of curing parameters validation testing will be dealt with in an overview manner.

Results of spring-in investigations performed at the DLR Institute of Composite Structures and Adaptive Systems will be presented. They are based on parameter determinations by means of experimental testing and the application to a relevant airframe structure.

Nomenclature

$\alpha_{m_{chem}}$ chemical matrix shrinkage $[1/K]$
$\alpha_{m_{equ}}$ equivalent matrix shrinkage $[1/K]$
$\alpha_{m_{therm}}$ thermal matrix shrinkage $[1/K]$
α_R radial CTE $[1/K]$
α_T tangential CTE $[1/K]$
ϕ_R radial chemical shrinkage $[\%]$
ϕ_T tangential chemical shrinkage $[\%]$
θ nominal structure angle $[Deg]$
ΔT process temperature difference $[K]$
ΔV_{chem} chemical volume shrinkage $[\%]$
$\Delta\theta$ spring-in angle $[Deg]$

1 Introduction

Due to their superior mechanical and mass characterisics besides other advantages compared to conventional materials, fiber reinforced composites are increasingly used for airframe structures. This comes with the side effect that in the manufacturing process internal stresses and hence deformations may be induced. The internal stresses may additionally be amplified due to assembly constraints and in-service loads. Taking into account manufacturing cadences of more than 30 aircraft/month economic processes are mandatory. This implies a high quality wrt. the mechanical performance (to avoid scrap parts) and geometrical shape conformance (to avoid higher assembly costs caused by efforts like shimming or expensive assembly equipment). The trend towards the production of highly integral structures may on the one hand elliminate assembly costs to a certain extent but may on the other hand require more sophisticated processes in the manufacturing.

Therefore analysis methods and strategies are required to predict the material characteristics and thereby enabling the simulation of manufacturability and behaviour of composite structures after assembly and in service. It starts with curing problems in manufacturing, where internal stresses and deformations are induced by the chemical matrix shrinkage and the un-isotropic CTE (*Coefficient of Thermal Expansion*) of such materials. A formation of additional stresses is

caused by assembly of the distorted parts in nominal mounting position. And finally there are in-service loads which may have to be added to prior introduced loads and may lead to lower load bearing capabilities as predicted, hence overloading the structure (see Fig. 1).
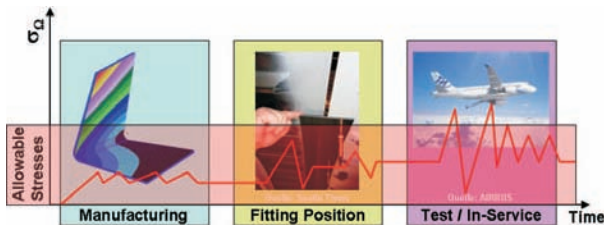
Fig. 1 Internal and external structural loads

In the above explained context the thermal analysis plays a central role in structure design (see Fig. 2). For the simulation of the curing it is necessary to predict transient temperature fields taking into account volumetric heat sources coming from chemical reactions of the matrix material. It is the basis for the determination of the degree of cure and hence the chemical shrinkage. Together with this comes the aspect of the interaction between manufactured part and tooling, especially when CTEs between both are not compatible. The optimization of the curing cycle (temperature levels, heating and cooling rates) can induce or may avoid residual stresses. It has in the following an impact on the in-service predictions e.g. margins of safety. With accurate simulation methods the save prediction of this phenomenon will help establishing reliable manufacturing processes, which may also lead to a reduction of margins of safety and to the reduction of necessary validation and testing effort.

The process parameters have a big influence on the chemical matrix shrinkage during transformation from liquid to solid state. Therefore scientists combined curing, thermal and residual stress analysis. Svanberg and Holmberg [1] developed a visco-elastic material model taking into account relaxation of the matrix in rubbary state and established a link to the thermal analysis. A similar strategy was proposed by Zhu and
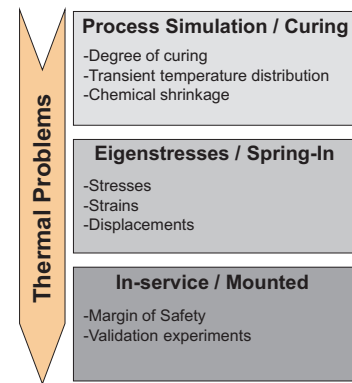
Fig. 2 Thermal issues in the manufacturing chain

Geubelle [2]. The link to the residual stress analysis is possible since the chemical shrinkage can directly be related to the degree of cure. Flores [3] compared several models for this relation and evaluated their application.

Other approaches were proposed by Darrow [4] and Sweeting [5] who simulated the spring-in on angled structures based on a linear-static FE-analysis. Darrow used an equivalent CTE for the matrix material combining thermal and chemical shrinkage properties. Sweeting accounted for the thermal expansion by using the CTE but applied the chemical matrix shrinkage as prescribed strains. In the present work, which summarizes spring-in investigations of the DLR Institute of Composite Structures and Adaptive Systems, the strategy proposed by Darrow [4] is pursued.

For the optimization of the whole manufacturing process it is necessary to consider curing and mechanical analysis. However, it has already been shown, that a fast engineerlike spring-in estimation based on linear-static analysis with added chemical shrinkage of the matrix is a reasonable approach. The drawbacks to a combined analysis are that it requires:

1. a sample test programm for each material and process,
2. that the structure will be manufactured with same process as the sample test programm,
3. the assumption that the whole structure is homogeneously cured.

2 Identification of Material Parameters

2.1 General Remarks

The determination of the magnitude of the matrix shrinkage was performed based on CFRP (*Carbon Fiber Reinforced Plastic*) L-profiles as shown in Fig. 3. This kind of structure was chosen, since it has already been closely investigated. It is therefore well described in literature and analytical formulas for verification exist.
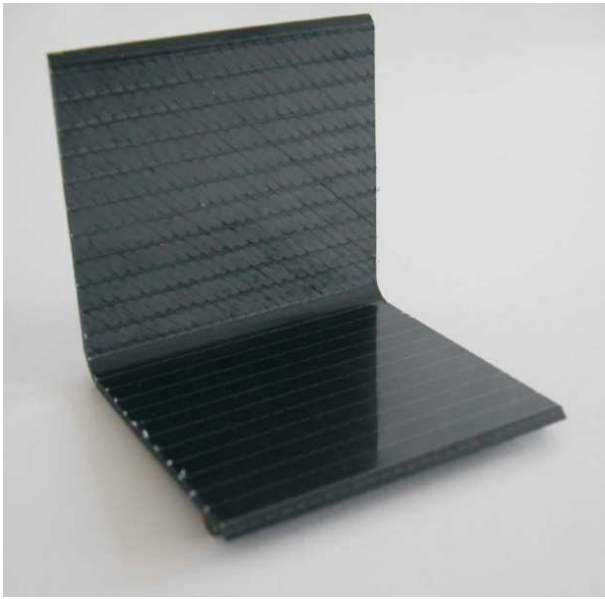
Fig. 3 CFRP L-profile test specimen

Main reason for spring-in on a L-shaped structure is the different shrinkage (chemical and thermal) in radial and tangential direction. Assuming the radial shrinkage to be much higher than tangential, shrinkage will cause outer fibers to move to smaller radii and inner fibers to move to larger radii as depicted in Fig. 4. This leads to compression in the outer fibers and tension in the inner fibers. Assuming furthermore, that the fibers are sufficiently stiff, a certain spring-in angle θ will be generated.

Radford and Rennick [7] derived an analytical equation for the determination of the spring-in on angled structures made from orthotropic material. Herein Δθ being the spring-in angle, θ the original structure angle (90° in the present
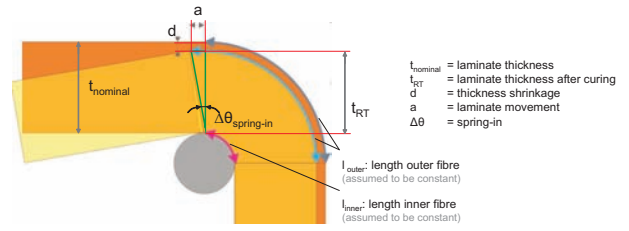
Fig. 4 Principle of spring-in mechanism [6]

study), α_T, α_R and ϕ_R, ϕ_T the tangential and radial shrinkage (thermal and chemical) and ΔT the process temperature difference.

$$\Delta\theta = \theta \left\{ \left[\frac{(\alpha_T - \alpha_R) \cdot \Delta T}{1 + \alpha_R \cdot \Delta T} \right] + \left[\frac{(\phi_T - \phi_R)}{(1 + \phi_R)} \right] \right\} \tag{1}$$

Dealing with fiber-composite materials requires to know the parameters of the single constituents. The laminate of the L-profile in this study consists of HTS-fibers from TOHO/TENAX and the RTM6 matrix system from HEXEL. All data were taken from literature [8]-[14]. The parameters of a uni-directional single ply are calculated using ESAComp3.4. As a reference a laminate with a FVF = 60% (*Fiber Volume Fraction*) is considered. All data are listed in Table 1.

Table 1 Material properties of HTS/RTM6 unidirectional single ply

Properties	Value	Unit
E_{11}	143 960	N/mm^2
$E_{22} = E_{33}$	5 955	N/mm^2
$G_{12} = G_{13}$	2 485	N/mm^2
G_{23}	2 235	N/mm^2
$\nu_{12} = \nu_{13}$	0.26	–
ν_{23}	0.33	–
Density ρ	1 512	kg/m^3

Since the CTE of the constituents turned out to be the most unreliable data, a study investigating their influence on the spring-in behaviour was conducted. It could be shown, that the CTE of the matrix dominates the mechanical behaviour of

the laminate. For the study this paramter will be considered as unknown and has to be determined such that the correct spring-in will be simulated. In the following this parameter is named equivalent CTE and is defined as sum of thermal and chemical shrinkage related to the process temperature difference (see Equation (2) taken from [15]).

$$\alpha_{m_{equ}} = \alpha_{m_{therm}} + \alpha_{m_{chem}} = \alpha_{m_{therm}} + \frac{\Delta V}{3 \cdot \Delta T} \quad (2)$$

Four different processes were investigated. All leading to a temperature difference of $\Delta T = 160K$ coming from $180°C$ highest process temperature and $20°C$ room temperature.

P1 (nominal) - gelation $130°C$ / curing $180°C$

P2 (max shrink) - gel. / cure $180°C$

P3 (mid shrink) - long gel. $130°C$ / cure $180°C$

P4 (low shrink) - long gel. $110°C$ / cure $180°C$

P1 is a nominal industrial process. P2 is the process with the highest shrinkage, since a fast gelation at high temperature prevents a shrinkage compensation by liquid resin. Processes P3 and P4 have a lower shrinkage due to their long gelation time a lower temperatures. This is caused by the slow change from liquid to solid state allowing the compensation of the shrinkage by liquid resin. As assumption the process P4 is considered as a process without chemical shrinkage which means, that the equivalent CTE has a thermal term only.

2.2 L-profile FE-Modell

To properly predict the spring-in it is mandatory to account for the thickness effect as it is described in chapter 2.1. Hence the L-profile was modelled with solid (HEX8) elements using MSC/Patran (see Fig. 5). The test structures were made from a 2*mm* laminate with 8 NCF (*Non-Crimp Fabric*) single plies ($t = 0.125mm$) and a symmetrical lay-up of $[4 \times \pm(45°)]$. The inner radius of the L-profile is 5*mm*.

In the FE model each single ply needs to be modelled with at least 3 elements over its
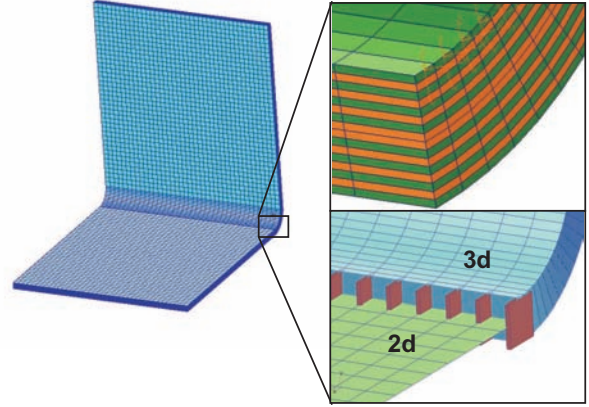
Fig. 5 CFRP L-profile FE-modelling

thickness. With this requirement and in order to avoid elements with bad aspect ratios an extremely fine mesh is required leading to an enormeous number of DoF (*Degrees of Freedom*) even for comparably small structures like the L-profile. Therefore the capability of a hybrid modelling was investigated. In this case the thickness effect is accounted for by using HEX8 elements (3D-orthotropic material) only locally in the zone of the radius. The remainders of the structure are modelled with QUAD4 shell elements (2D-orthotropic material) as can be seen in Fig. 5. This leads to the reduction of the DoF enabling the analysis of large, thin-walled composite structures. The interface between solid and shell elements is modeled with stiff bar elements to prevent warping at the free edges of the solid area.

In this study each structure was analyzed under two different conditions. First, iso-static mounting to obtain free internal stresses and the corresponding deformations. Second, in in-service mounting conditions to calculate stresses in superimposed condition of internal and mounting loading.

2.3 L-profile FE Analysis and Results

In the analyses the matrix CTE was adjusted such, that the spring-in angles are equal to the experimentally gained ones for a FVF = 60%. All

other FVF from 55% to 70% were conducted to check the reliability of the method. In Fig. 6 there are shown measured and analyzed spring-in angles related to the norm process P1 and a FVF = 60%. As previously defined the process P4 shall be a zero-chemical shrinkage process. Based on this the chemical volume shrinkage for the processes P2 - P4 varies between $0.68\% \leq \Delta V_{chem} \leq 3.25\%$. The corresponding shrinkage parameters namely the equivalent CTEs in fiber direction and perpendicular direction vary between

$0.08 \cdot 10^{-6} K^{-1} \leq \alpha_{11} \leq 0.630 \cdot 10^{-6} K^{-1}$ and $36.80 \cdot 10^{-6} K^{-1} \leq \alpha_{22}, \alpha_{33} \leq 63.27 \cdot 10^{-6} K^{-1}$.
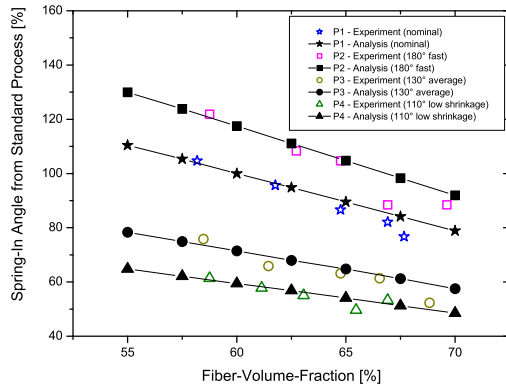
Fig. 6 Comparison of measured and calculated spring-in results

The results coming from equation (2) by using the gained shrinkage data of a uni-directional single ply leads to approx. 25% lower spring-in results as experimentally measured. Even by using the pure thermal CTE for P4 the results do not lead to comparable values. The experimentally measured values of the spring-in however correspond to data gained by Darrow [4]. The spring-in results gained by using the hybrid FE modelling are in very good agreement with the fully 3D modelled L-profile. It therefore is considered to be suitable for the analysis of a large, thin-walled composite structure.

In terms of stresses the process P2 resembles the process with the highest chemical shrinkage and hence highest eigenstresses. Under iso-static

mounting conditions the matrix has a tension load of $\approx 68N/mm^2$ and it follows trivially that the fibers have a compression load of the same magnitude. In fixed configuration the stresses are ranging from $-158N/mm^2$ in the fibers of the outer radius and $\approx 66N/mm^2$ in the matrix of all layers. Here the gained results need some more discussion. Especially the magnitude of tensile strength in the matrix system needs to be investigated more thoroughly. As a remark it shall be mentioned, that the induced stresses in the nominal process P1 are about half of the before described P2.

3 Analysis of Curved Airframe Structure

3.1 General Remarks

For a spring-in analysis of a large, thin-walled structure is becomes obvious, that a full solid modelling is not manageable in terms of model sizes and hence computational effort. Therefore the idea of hybrid modelling is transferred from L-profile level to a larger airframe structure. All material properties determined within the L-profile investigations are used for this large scale application which is, stiffness and shrinkage properties as outlined in previous paragraphs. As a measure of the analysis results the computed spring-in of the global radius of a curved Z-profile as shown in Fig. 7 were compared to experimentally gained data.

3.2 FE-Model of Curved Airframe Structure

A Z-shaped generic frame structure with a global curvature radius of $\approx 2m$, a length of $\approx 2.5m$ and a variable profile height between $90mm$ and $120mm$ was subject of the investigations as depicted in Fig. 7. The same material properties as for the L-profile are used and the profile is manufactured according to process P1, the norm process. The web is composed of 8 uni-directional single plies with a thickness of $t = 0.25mm$ and a $[2 \times (\pm 45)]_S$ lay-up. 13 plies are foreseen alternatively in the inner and outer chord with a lay-up of $[(+45/-45/0)_S/0/(+45/-45/0)_S]$ and a total thickness of 3.25mm.
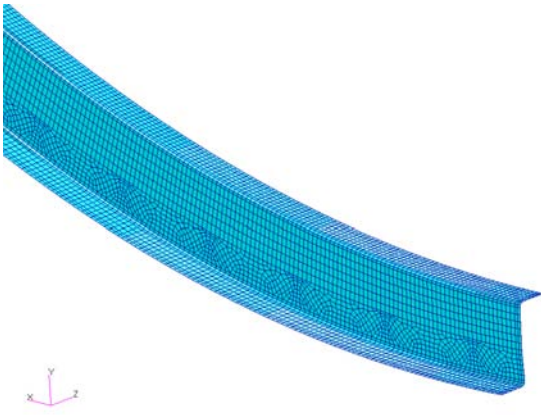
Fig. 7 Curved frame Z-profile

In order to determine the free eigenstresses and the global spring-in the Z-profile was isostatically fixed at one free end. Therewith avoiding that the web can not change its global orientation and no additional stresses are induced (see Fig. 8 left). The fixation in in-service position is such, that the outer chord can move along the circumferential line of the global radius but all other movements are prevented as can be seen on the right picture of Fig. 8.
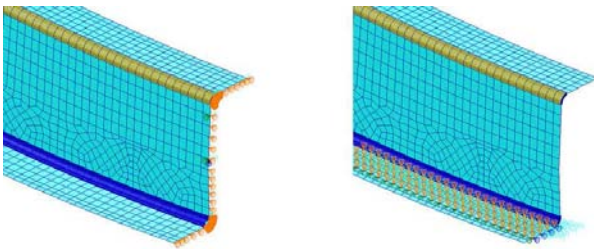
Fig. 8 Mounting of Z-frame for spring-in analysis

As earlier mentioned the pure 3D modelling leads to a very high number of DoFs already for comparably small structures. Therefore three different model types were analysed and evaluted:

1. Model created from shell elements: Assuming that global spring-in is driven by shrinkage of the web, representing the transversal shrinkage and thereby forcing the belts to move to other radii which causes the spring-in effect.

2. Hybrid model with solid elements between web and inner chord: Assuming the same effect as in 1. and by consideration of the spring-in in the radius between web and inner chord.

3. Hybrid model with solid elements between web and both chords: Assuming the same effect as in 1. and by consideration of the spring-in in both radii between web and chords.

3.3 Z-profile Analysis and Results

In this section there are shown the analysis results in terms of spring-in of the global profile radius and stresses. The principle behaviour of the investigated structure wrt. to its lay-up in the inner and outer chords is shortly discussed.

Figure 9 shows the Z-profile with a slightly decreased global radius together with some torsion of the profile. This mode will occure with unidirectional layers in either both chords or only in the outer chord. In case of unidirectional layers in the inner chord this kind of profile would "spring-out" due to different CTE between inner and outer chord. The inner chord with its low CTE and high stiffness would remain almost unchanged whereas the outer chord with its high CTE would open the curved structure.

The before mentioned three different ways of modelling the generic frame structure with different considerations of the relevant spring-in zones were investigated at first. It became obvious, against expectations, that the global spring-in is driven by the local spring-in in the radii between web and chords. This holds especially true, if there are longitudinal layers foreseen in the chords, which provide a high stiffness and low shrinkage in profile longitudinal direction. In case there are no longitudinal layers foreseen in a chord it may be possible the save a 3D modelling in this zone but it depends very much on the design of the structure and the chosen material. However, all results that will be presented hereafter are gained from a model considering all local thickness effects.
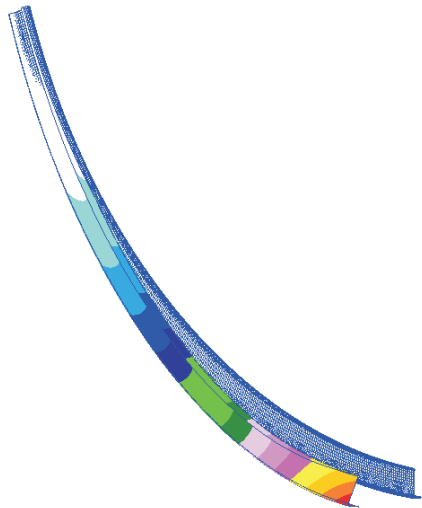
Fig. 9 Deformed shape of Z-profile after manufacturing

In Table 2 there are listed the global spring-in radii, that where analyzed with the different process parameters, as well as the global spring-in radius of the manufactured part using process P1. It can be seen, that the data fit quite well with the measured ones. Furthermore, it becomes obvious that the difference between the processes P1 (nominal) and P2 (fast) is smaller than comparing P1 with P3 and P4. In case of the last-mentioned a more significant decrease of spring-in can be noticed compared to P1. This seems advantageous from quality point of view but these processes require 1.5 to 2 times longer process times, which on the other hand is disadvantageous in the sense of the achievement of high manufacturing rates.

In the following Table 3 all stresses gained from the iso-static configuration are listed for processes P1 and P2 for comparison. Hereby the the stresses are evaluated in fiber and matrix direction and distinguishing also between chords and frames. It can be noticed that the stresses in the matrix material correspond to the values that were determined during the L-profile investigations. In most parts of the Z-profile the same can also be noticed for the fiber compression loads.

Table 2 Spring-In of global radius of curved airframe structure

Process	Global Radius	Difference to norm Process
produced (P1)	1963.5 *mm*	0.0 *mm*
P1	1964.5 *mm*	1.0 *mm*
P2	1963.0 *mm*	-0.5 *mm*
P3	1967.1 *mm*	3.6 *mm*
P4	1968.9 *mm*	5.4 *mm*

In the radii between web and chords the stresses are slightly increased and in $\pm 45°$ fibers of the inner chord a distinctive raise in the stresses becomes obvious. This is due to the specific deformation caused by the profile shape and of course due to the un-isotropic material. Comparing furthermore the magnitude of stresses between the two processes it is noticable, that the stresses of P2 are about twice as high as for the norm process. In the specific case of P1 and P2 the process times were equal. This underlines the high dependency of internal stresses from the way of curing.

Table 3 Induced residual stresses in fiber and matrix

Stresses [MPa]		P1		P2	
		Min	Max	Min	Max
Fiber	Chords	-63	33	-125	65
	Frame	-33	53	-65	102
Matrix		30	34	58	70

All stresses that were analyzed with the structure mounted in its in-service position show only marginal changes in the order of $\pm 3 N/mm^2$. The changes of the stresses are once again very much dependent on the design of the structure and also on its mounting conditions. This becomes obvious when comparing the calculated low values of the generic frame structure with the results of the L-profile which are decisively larger.

It should be mentioned that the calculated matrix stresses even for the norm process P1 are extremely close to typical failure loads of epoxy resins. This topic needs more detailed investigations to allow save design under consideration of manufacturing issues. One way of investigating the severity, could be the monitoring of micro cracks after demoulding.

4   Outlook

In order to enable a full simulative design taking into account all aspects from manufacturing to in-service a reliable curing simulation and structure validation has to be established.

This virtual method of process simulation is considered to be very promising to initially predict the component properties (degree of cure, residual stresses and deformations) for a given cure cycle. Moreover, it provides a basis for a comprehensive process optimization to minimize cycle times regarding allowable stresses and deformations. In order to provide numerical models for cure simulation and make them ready for industrial application, research is conducted in different fields.

At first, the reaction kinetics of thermoset materials is characterized. Standard DSC (*Differential Scanning Calorimetry*) and Rheometer measurement systems (see Fig. 10) are applied to determine the glass transition temperature and viscosity of the resin as a function of cure temperature and cure degree. The obtained measurement data are also studied for extended interpretations, e.g. to estimate the gelation point. Thereupon common kinetic models are enhanced for selected resin systems, and techniques are developed to derive their associated parameters (see Fig. 11).

Secondly, these curing models are implemented into commercial finite element software. When applying this simulation method, the influence of relevant boundary conditions, such as the temperature distribution within RTM moulding tools, can be investigated by analyzing the computed temperature fields and fields of degree of cure as can be seen on a neat resin example
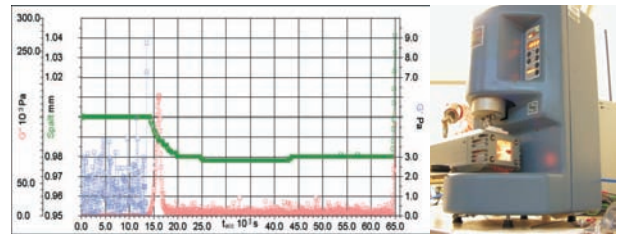
Fig. 10 Matrix gelation time measurements
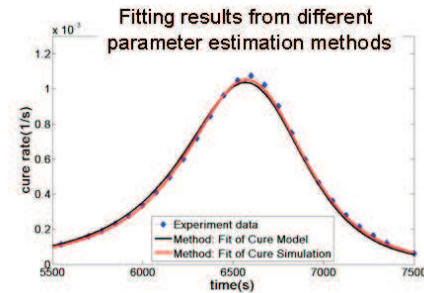
Fig. 11 Curing parameter optimization

in Fig. 12. In order to optimize the tool shape and energy application for relevant components, optimization procedures can be applied to reach minimum process time while avoiding an overheating as well as assuring uniform distributions of temperature and degree of cure.
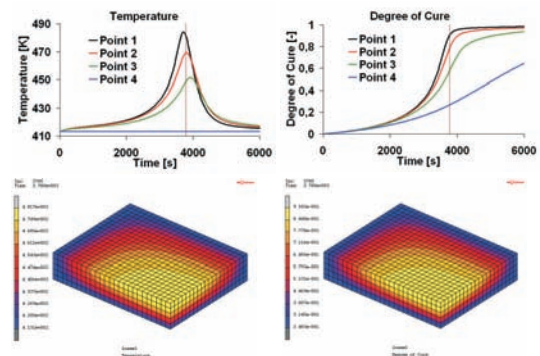
Fig. 12 Neat resin cure simulation - degree of cure

Further research will focus on the coupled thermo-kinetic-mechanical simulation of cure stresses and deformations (e.g. spring-in) as well as their validation against experimental results. Within this context, the determination of cure

shrinkage and mechanical properties as functions of temperature and degree of cure need to be conducted, and investigations on appropriate methods for stress measurement are a great challenge.

Furthermore thermal properties like heat conductivity and capacity and mechanical properties like Young's modulus, density or creep behavior are mandatory. All these properties are dependent from temperature leading to highly nonlinear problems.

A variety of curing models already exists. These models need to be enhanced or adapted to their specific use. Herein each matrix material requires its own laborious identification of necessary parameters in order to adequately determine the variables of the curing models.

Finally, for testing of composite structures subjected to combined mechanical and thermal loads DLR uses its thermo-mechanical testing facility named THERMEX. It allows for the simultaneous application of thermal loads with a temperature gradient of up to $1200K$ and a tension or compression loading up to $400kN$ on structures with a size of about $1m$ x $0.8m$.

Fig. 13 THERMEX - thermo-mechanical test facility

5   Summary

A way is presented which allows for the determination of spring-in deformations and eigenstresses of large, thin-walled CFRP structures based on linear-static FE simulations. Furthermore this approach allows for the prediction of stresses inside the structures in mounted position including prior determined eigenstresses. All analyses within this study are performed using MSC/Nastran.

All mechanical properties of the single laminate constituents were extracted from literature and the properties of the unidirectional single plies were analysed using ESAComp3.4. Thermal and chemical shrinkage were determined by comparing test results on CFRP L-profiles with analysis results based 3D FE models representing each single layer of the structure. Test results gained from the process with low chemical shrinkage were used to determine the thermal contribution to the spring-in. For the remaining three tests the contribution of the chemical shrinkage was determined. The L-profile was re-analysed for a number of different fibre-volume fractions for validation reason. The outcome in terms of displacements showed very good agreement with the test results. Concerning eigenstresses, comparably high values were found for the matrix material.

The used kind of modelling leads to very large FE models. Therefore a simplification which combines 2D and 3D modelling was introduced. Those parts, where the transversal CTE leads to spring-in, are modelled conventionally using solid elements. All remaining parts, which are mainly flat, are modelled using shell elements. The application to the L-profile showed reasonable agreement and therefore this modelling technique was transferred to the simulation of a generic frame structure.

Studies with different modelling of the Z-profile showed that an adequate consideration of the radii between belts and web by 3D modelling are mandatory for reliable deformation predictions on large, thin-walled structures.

In conjunction with the presented work there are further steps in the frame of process simulation. First there is the establishment of a curing simulation to determine the degree of cure and chemical shrinkage. This has to be realized in conjunction with the consideration of thermal analysis to take into account exothermal reactions and other transient thermal aspects during the

processing of parts inside manufacturing tools. Finally, these two disciplines need to be combined with the mechanical analysis. This compendium of different disciplines would, as direct consequence, provide an integrated tool for the simulation of fibre-composite parts from manufacturing up to in-service behaviour.

References

[1] Svanberg J. Magnus and Holmberg J. Anders. Prediction of shape distortions, Part 1. FE-implementation of a path dependent constitutive model. *Composite Part A: Applied Science and Manufacturing*, Vol. 35, Issue 6, June 2004, pp 711-721

[2] Zhu Qui and Geubelle Philippe H. Dimensional accuracy of thermoset composites: shape optimization. *Journal of Composite Materials*, Vol. 36, No. 6, 2002, pp 647-672

[3] Flores F., Gillespie Jr. J.W. and Bogetti T.A. Experimental investigation of the cure-dependent response of vinyl ester resin. *Polymer Engineering and Science*, Vol. 42, No. 3, March 2002, pp 582-590

[4] Darrow A. David. Isolating components of processing induced warpage in laminated composites. *Journal of Composite Materials*, Vol. 36, 2002, pp 2407-2419

[5] Sweeting R., Liu X.L. and Paton R. Prediction of processing-induced distortion of curved flanged composite laminates. *Journal of Composite Structures*, Vol. 57, 2002, pp 79-84

[6] Sproewitz T., Kleineberg M. and Tessmer J. Prozesssimulation in der Faserverbundherstellung – Spring-In. *NAFEMS Magazin Newsletter*, 1/2008, 9. edition

[7] Radford D.W. and Rennick T.S. Separating sources of manufacturing distortion in laminated composites. *Journal of Plastics and Composites*, Vol. 19, No. 8, 2000, pp 621-641

[8] Hexel Corporation. Product Sheet HexFlow RTM6 - $180°C$ epoxy system for resin transfer moulding monocomponent system

[9] Svanberg J. Magnus. Prediction of shape distortion for a curved composite C-spar. *Journal of Reinforced Plastics and Composites*, Vol. 24, No. 3, 2005, pp 323-339

[10] Hobbiebrunken T. Thermomechanical analysis of micromechanical formation of residual stresses and initial matrix failure in CFRP. *JSME International Journal*, Series A, Vol. 47, No. 3, 2004, pp 349-356

[11] Holmberg J.A. Resin transfer moulded composite materials. Doctoral Thesis, *LuleåUniversity of Technology*, Department of Materials and Manufacturing Engineering, Division of Polymer Engineering, Report 1997:10, 1997

[12] TOHO TENAX Europe GmbH. Produktprogramm und Eigenschaften für TENAX® HTA/HTS Filamentgarn

[13] Hull D. *An Introduction to Composite Materials*. University Press, Cambridge 1988

[14] http://www.torayca.com/techref/

[15] Callister W.D. *Material Science and Engineering an Introduction*. 3. edition, 1994

Copyright Statement